

*Short Communication*

## **Aluminum Chloride Reveals the Catalytic Activity Towards Laser-Induced Deposition of Copper from Water-Based Solutions**

*Olga A. Lozhkina<sup>\*</sup>, Maxim S. Panov, Lev S. Logunov, Ilya I. Tumkin, Dmitry I. Gordeychuk, Vladimir A. Kochemirovsky*

Institute of Chemistry, Saint-Petersburg University, 198504 Saint-Petersburg, Petrodvorets, 26 Universitetsky, prosp., Russian Federation.

\*E-mail: [lasergroupspb@gmail.com](mailto:lasergroupspb@gmail.com)

*Received: 10 April 2015 / Accepted: 29 May 2015 / Published: 24 June 2015*

---

Catalytic actions of aluminum chloride on laser-induced liquid-phase copper deposition process were studied. Copper deposition experiments in aqueous solutions containing aluminum chloride upon 532 nm laser irradiation at different line deposition rate were performed. The influence of pH on the deposition rate and topology of the deposited copper microstructures was investigated. Enhanced rate of copper reduction in aluminum chloride solutions was observed. High purity copper microstructures with good electrical conductivity were obtained.

---

**Keywords:** laser-induced deposition, copper, solution, electrical resistance, microelectronics, aluminum chloride

### **1. INTRODUCTION**

One of the promising techniques for patterning of the microelectronic devices is laser-induced chemical liquid-phase deposition of metals (LCLD). In this method the metal reduction reaction proceeding in local volume of solution in the vicinity of the laser beam focal point results in deposition of metal microstructures (lines) on the surface of dielectric substrate. Thus, laser-induced deposition of such metals as copper, silver [1], palladium [2], platinum [3], nickel [4], gold [5], chromium and tungsten [6] can be used for fabrication of extra small metallic conductors on dielectric surfaces without using photomask in contrast to photolithography [7-13]. It should be pointed out that in the aforementioned series copper attracts more attention due to its wide application in microelectronics and high catalytic activity of nanoparticles based on this metal [14,15]. However, the relatively low

deposition rate of metal lines significantly complicates the practical implementation of LCLD. For example, the typical deposition rate of copper line is  $2.5 \mu\text{m s}^{-1}$  [16-20], therefore it takes more than one hour in order to produce microconductor with length of just 10 mm. On the other hand, laser-induced copper deposition at higher rates results in formation of the microstructures with a poor topology. Thus, increase of the deposition rate of metal lines and concurrent preservation of the topology of the corresponding deposited metallic microstructures provide conditions for more efficient utilization of LCLD technique.

In previous studies it was shown that introducing organic additives or changing a reducing agent [21] as well as using a substrate as a reducing agent [22] may lead to topology improvement of the deposited metallic microstructures. However, for instance, laser-induced deposition of copper from solution containing organic components is accompanied by side reactions [23], and moreover also proceeds only at low rate of line deposition. In addition, there are few publications in which the implementation of the additives containing metal salts in laser-induced copper deposition process was studied in some detail [24-26]. In turn, the action of these additives on the line deposition rate has not yet been discussed and remains uncertain. In this report we study influence of aluminum chloride additive on the copper line deposition rate and topology of the deposited copper microstructures.

## 2. MATERIALS AND METHODS

The copper lines were deposited from solution **1-5** (Table 1) on the surface of glass-ceramics (Sitall ST-50-1) upon irradiation at 532 nm. Sitall ST-50-1 as the crystalline glass-ceramics material is widely applied in microelectronics and composed of  $\text{SiO}_2$  (60.5%),  $\text{Al}_2\text{O}_3$  (13.5%),  $\text{CaO}$  (8.5%),  $\text{MgO}$  (7.5%) and  $\text{TiO}_2$  (10.0%). All chemicals used for preparation of **1-5** were of analytical grade (Sigma-Aldrich). In these solutions xylitol, sodium hydroxide, sodium potassium tartrate tetrahydrate and aluminum chloride were used as a reducing agent, acidity regulator, ligand and additive, respectively. We used xylitol as reducing agent due to its recent successful application in laser-induced deposition of copper from water-based solutions [27].

**Table 1.** The composition of solutions used for LCLD of copper.

solution	concentration ( $\text{mmol L}^{-1}$ )				
	$\text{CuCl}_2$	$\text{KNaC}_4\text{H}_4\text{O}_6 \times 4\text{H}_2\text{O}$	$\text{NaOH}$	$\text{C}_5\text{H}_{12}\text{O}_5$	$\text{AlCl}_3$
<b>1</b>	10	33	100	75	0.0
<b>2</b>	10	33	100	75	0.1
<b>3</b>	10	33	100	75	0.3
<b>4</b>	10	33	100	75	1.0
<b>5</b>	10	33	100	75	3.0

The detailed description of the experimental setup for LCLD has been published elsewhere [19]. The output from a continuous wave 532 nm diode-pumped solid-state Nd:YAG laser is split into two parts. One is focused on the boundary region between metal salt solution and dielectric substrate which are placed on computer controlled motorized stage used for adjustment the focal point position

where the deposition reaction is supposed to start. Second is sent to web-camera used for in situ monitoring and control of the laser-induced deposition process. Laser-induced deposition of copper from 0.5 mm thick solutions was performed at different laser power (from 500 to 1000 mW) and line deposition rates were 2.5, 10, 20 and 30  $\mu\text{m s}^{-1}$ . Optical images of copper lines were obtained using an optical microscope with 20 $\times$  magnification (MMN-2, LOMO). The topology of the deposited copper-containing microstructures was observed by means of scanning electron microscopy (SEM). The atomic composition of these microstructures was studied using energy dispersion of X-ray spectroscopy (EDX). The EDX-system was coupled with a Zeiss Supra 40 VP scanning electron microscope equipped with X-ray attachment (Oxford Instruments INCA X-act). The electrical conductivity properties of the deposited copper lines were studied with an impedance meter Z-2000 (Elins Co.) in the frequency band of 20 Hz to 2 MHz at the signal amplitude of 125 mV.

### 3. RESULTS AND DISCUSSION

In order to optimize copper deposition process from solutions **1-5** (Table 1) and determine initiation threshold, i.e. minimum laser radiation density value at which deposition of copper microstructures starts, the laser output power was varied from 500 to 1000 mW. The dependence of copper line width on laser power is demonstrated in Fig. 1a.

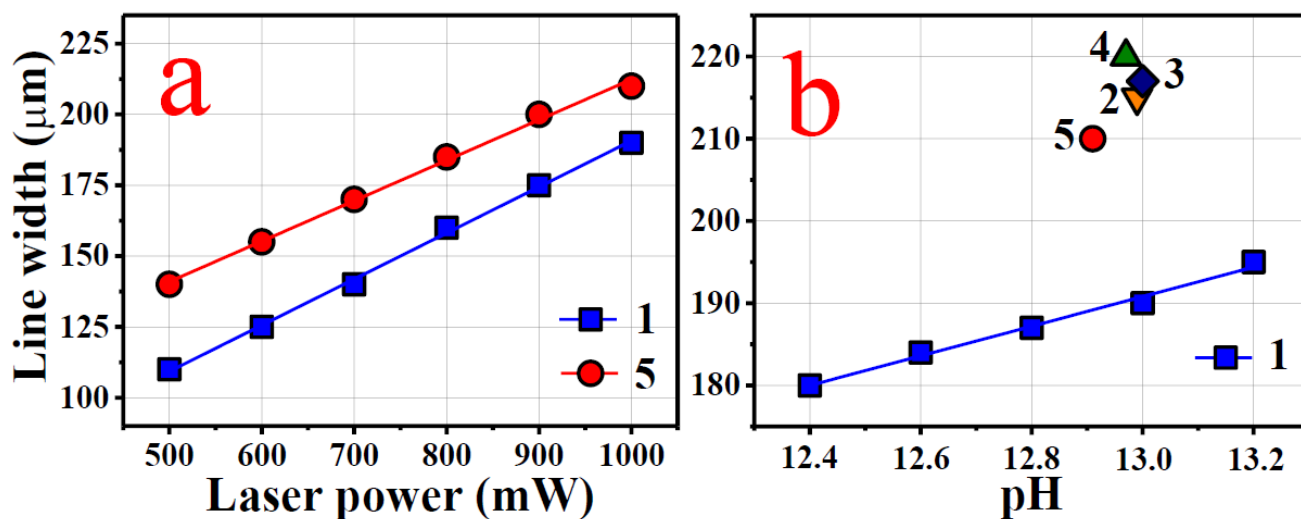


**Figure 1.** The width of copper lines as a function of laser power (a) and as a function of pH (b). LCLD from solutions **1-5** was performed at deposition rate of 30  $\mu\text{m s}^{-1}$ . All copper deposition experiments at different pH (b) were carried out at laser power of 1000 mW.

It was found that the microstructures deposited from **5** are wider than those obtained from **1**, in turn the width of all of them increases with the laser power increase. Here we do not show deposition results from other solutions containing aluminum chloride (**2-4**) because they exhibit no noticeable difference in the line width within the aforementioned range of laser power in comparison with LCLD results from **5**.

Optical microphotograph of typical copper line deposited from solution **5** at deposition rate of  $30 \mu\text{m s}^{-1}$  and laser power of 1000 mW is shown in Fig 2a. A specific electrical resistance of all deposited copper microstructures was calculated using equation (1) in order to estimate ability to conduct electricity.

$$\rho = \frac{R \times d \times l}{L} \quad (1)$$

where  $\rho$  is a specific electrical resistance,  $R$  – electrical resistance,  $d$  – width,  $l$  – thickness and  $L$  – length of copper lines deposited from **1-5**.

Electrical resistance was measured using impedance spectroscopy; SEM images of the surface fracture of copper lines were used to obtain geometric parameters of these microstructures. Fig 2b illustrates the fractured surface of copper line deposited from **5**. According to this microphotograph the average thickness of the copper layer and the average width of the copper line are approximately 12 and  $210 \mu\text{m}$ , respectively. Line length in all LCLD experiments was held constant at 10 mm. Experimental conditions and properties of the deposited copper microstructures are presented in Table 2.

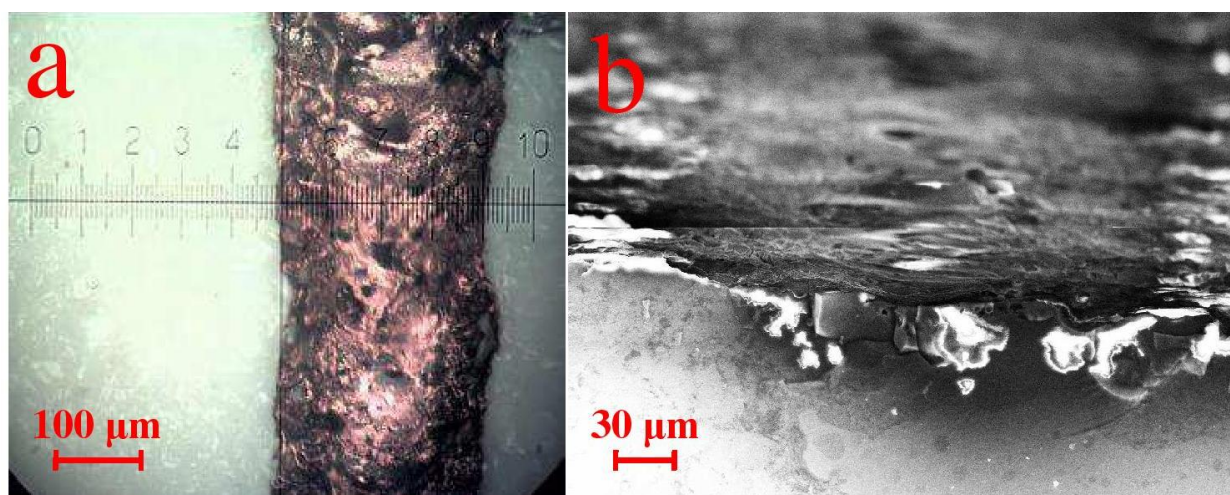


**Figure 2.** Optical microphotograph (a) and SEM image of the surface fracture (b) of typical copper line deposited from solution **5** at deposition rate of  $30 \mu\text{m s}^{-1}$  and laser power of 1000 mW.

Here it is clearly seen that the increase of the line deposition rate from  $2.5$  to  $30 \mu\text{m s}^{-1}$  results in a significant increase of a specific electrical resistance of the copper lines deposited from solution which does not contain aluminum chloride.

On the other hand, copper lines produced by LCLD from solutions containing aluminum chloride (**2-5**) exhibit low values of electrical resistance even at  $30 \mu\text{m s}^{-1}$  which is comparable with those revealed by copper line deposited from **1** at  $2.5 \mu\text{m s}^{-1}$ . Identical behavior was observed for LCLD products obtained from **2-5** at  $10$  and  $20 \mu\text{m s}^{-1}$ .

**Table 2.** Experimental conditions and properties of copper lines deposited from solution **1-5**.

solution	pH	laser power (mW)	line width $d$ ( $\mu\text{m}$ )	line deposition rate ( $\mu\text{m s}^{-1}$ )	specific electrical resistance $\rho$ ( $\Omega \text{ mm}^2 \text{ m}^{-1}$ )
<b>1</b>	13.00	1000	150	2.5	2.2
<b>1</b>	13.00	1000	190	30	56
<b>2</b>	13.00	1000	215	30	3.2
<b>3</b>	12.99	1000	217	30	3.0
<b>4</b>	12.97	1000	220	30	5.9
<b>5</b>	12.91	1000	210	30	4.5

Thus, the presence of aluminum chloride in the deposition solutions essentially affects the electrical conductivity properties of the copper microstructures. Low electrical resistance suggests that the topology of microstructures produced from solutions with aforementioned additive at higher rates of line deposition should have similar quality as those obtained from solutions without the presence of aluminum chloride at low rate of line deposition. Indeed, in Fig 3b, d SEM images demonstrate that copper lines deposited both from **1** and **5** consist of 40-120 nm particles and their agglomerates regardless of the aluminum chloride presence in solution. Analysis of the EDX spectra (Fig. 3a, c) shows that weigh percentage of copper is very high in both deposits and there is no presence of aluminum in microstructure deposited from **5**. Therefore it is reasonable to assume that aluminum chloride used as additive in LCLD experiments does not lead to co-deposition of aluminum and copper but results in formation of high purity copper microstructures even at higher line deposition rates. Although, a deeper understanding of the role of aluminum chloride in LCLD of copper of such high purity requires additional studies. Here, the major difficulty lies in the fact that the aforementioned problem is discussed for the first time and there are only few articles on similar topics. For example, R. J. Von Gutfeld et al. [24-26] showed that the photochemical processes can accelerate the laser-induced metal deposition. In his experiments the laser beam is focused at an interface between an copper electrode and solution of copper (II) sulphate. Second electrode was placed in solution, and then external voltage was applied to closed circuit. At small values of the external voltage it was possible to observe the jump of the potential  $E$ , of the order of 0.4 V at an interface between an copper electrode and solution of copper (II) sulphate upon laser irradiation which results in an increase of the rate of copper deposition within an irradiated area in 1000 times. R. J. Von Gutfeld et al have attempted to explain this effect only by thermal factor (kinetics of deposition) as well as by stirring the solution. However, simple calculations based on the Nernst equation indicate that the potential change in the solution induced by the heating can reach values of only 0.1-0.15 V. Moreover, the high thermal conductivity of copper revealed in the experiments mentioned above must facilitate the deposition of a wide copper structures, whereas in fact this behavior was not observed making the obtained results inconsistent with proposed idea of the copper electrodeposition within the local area of the laser beam.

In addition, it is well-known that aluminum chloride solution is hydrolyzed by sodium hydroxide forming hexacoordinated hydroxo complexes; in turn it makes the deposition solution less basic potentially resulting in improvement of the electrical conductivity properties of copper lines and increase of copper deposition rate. Thus, in order to shed light on this issue, we investigated the

influence of pH on the deposition rate and topology of copper microstructures. For that purpose, pH of solution **1** was varied by adjusting the sodium hydroxide concentration and measured with a glass electrode. On the other hand, it is very hard to measure such a small change in pH of solutions containing aluminum chloride, therefore the pH of **2-5** was calculated using equation (2).

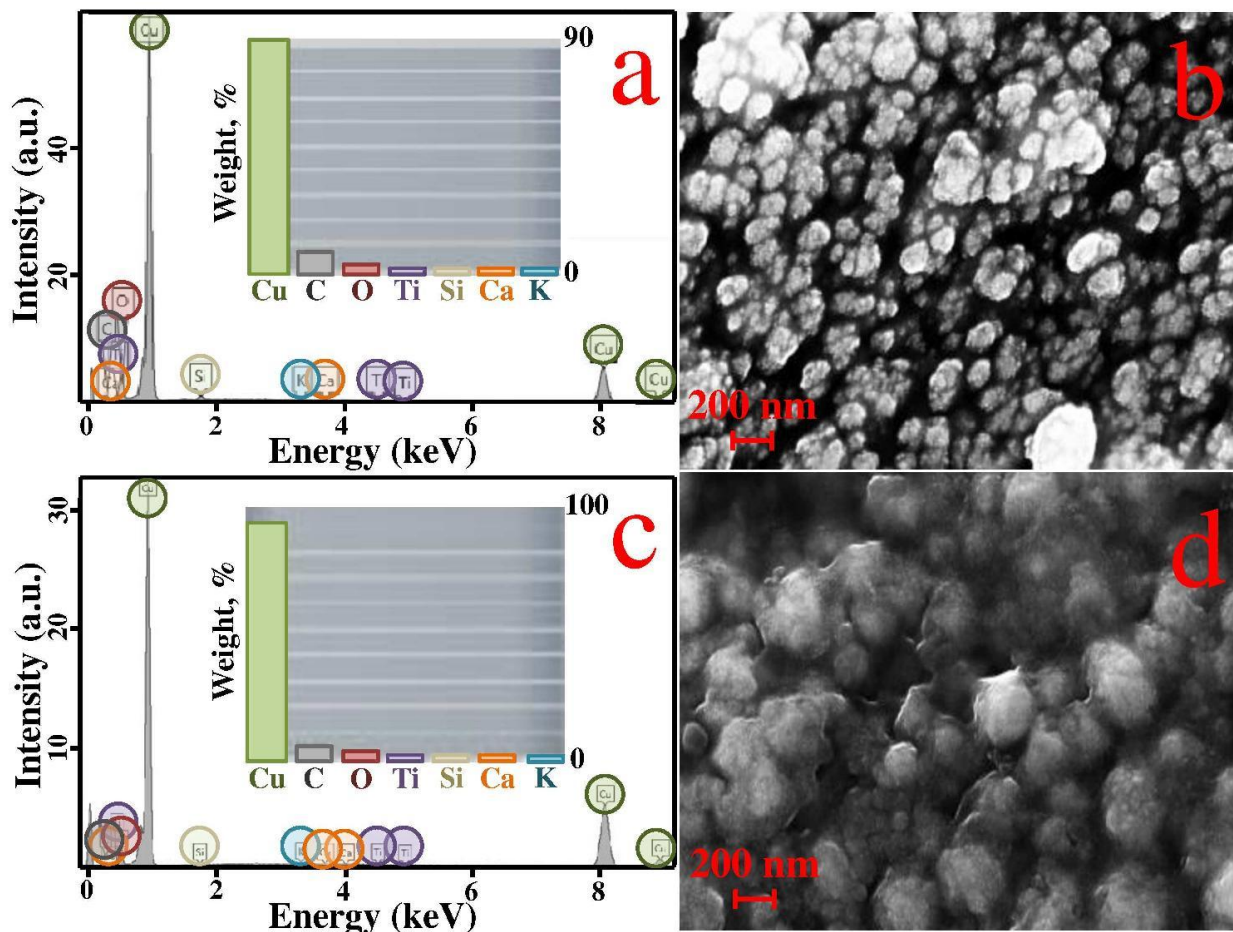


**Figure 3.** EDX spectrum (a) and SEM image (b) of copper line deposited from solution **1**. EDX spectrum (c) and SEM image (d) of copper line deposited from solution **5**. Weight percentage of all the elements found in the EDX spectra (a, c) are shown in the insets. LCLD from solutions **1** and **5** was performed at laser power of 1000 mW and at deposition rate of 2.5 and 30  $\mu\text{m s}^{-1}$ , respectively.

Moreover, it should be mentioned that aluminum hydroxide is completely soluble in the pH range studied and exists in solution as a negatively charged hexahydroxy complex; hence it does not take part in copper reduction reaction. The results of the aforementioned calculations are presented in Table 2.

$$\text{pH} = 14 + \lg([\text{NaOH}] - 6[\text{AlCl}_3]), \quad (2)$$

where  $[\text{NaOH}]$  and  $[\text{AlCl}_3]$  are concentrations of sodium hydroxide and aluminum chloride, respectively.

Fig. 1b illustrates the width of copper lines deposited from **1-5** as a function of pH. For **1** the line width dependence on pH is linear, thus one can estimate the copper line width exactly at the same

pH value calculated for 2-5. As a result, much narrower lines are produced from 1 even at pH corresponding to those calculated for solutions with aluminum chloride. Then, taking into account the fact that the metal line width is proportional to its deposition rate, one can assume that LCLD of copper from solutions containing aluminum chloride proceeds with higher rate.

#### 4. CONCLUSIONS

It was observed that aluminum chloride additives can significantly lower electrical resistance of copper lines and increase the rate of copper reduction in water-based solutions upon 532 nm laser irradiation. Catalytic nature of aluminum chloride in LCLD of copper was also supported by the results of energo-dispersive X-ray analysis. EDX spectrum of copper microstructure deposited from solution containing aluminum chloride at higher line deposition rate shows no aluminum signal whereas weight percentage of copper is more than 90%. Thus, we obtained high purity copper microstructures with good electrical conductivity properties at unusually high rate of line deposition thereby expanding the scope of application of LCLD technique in microelectronics.

#### ACKNOWLEDGEMENTS

We acknowledge the Russian Fund for Basic Research (grants 15-03-05139) and Saint Petersburg State University for a research grants (2015–2017, 12.38.219.2015) and postdoctoral fellowship (No. 12.50.1189.2014). The authors also express their gratitude to the SPbSU Nanotechnology Interdisciplinary Centre, Centre for Optical and Laser Materials Research, Centre for X-ray Diffraction Studies and Nanophotonics Centre, Centre for Geo-Environmental Research and Modelling (GEOMODEL).

#### References

1. J. H. G. Ng, M. P. Y. Desmulliez, A. McCarthy, H. Suyal, K. A. Prior, D. P. Hand, *UV direct-writing of metals on polyimide DTIP of MEMS and MOEMS* 360 (2008).
2. K. Kordás, J. Békési, R. Vajtai, L. Nánai, S. Leppävuori, A. Uusimäki, K. Bali, P. Moilanen, *Appl Surf Sci* 172 (2001) 178.
3. G. A. Shafeev, *Adv. Mater. Optics Electron.* 2 (1993) 183.
4. K. Kordas, J. Remes, S. Leppavuori, L. Nanai, *Appl. Surf. Sci.* 178 (2001) 93.
5. Yu. S. Tver'yanovich, V. A. Kochemirovsky, A. A. Man'shina, A. V. Povolotsky, A. V. Povolotskaya, S. V. Safonov, I. I. Tumkin, *Lazerno-indutsirovannoe Osazhdenie Zolota i Medi iz Rastvorov* (Laser-Induced Chemical Liquid Phase Deposition of Gold and Copper) St Petersburg: A S Pushkin Leningrad University (2010).
6. H. Yokoyama, S. Kishida, K. Washio, *Appl. Phys. Lett.* 44 (1984) 755.
7. R. Nowak, S. Metev, G. Sepold, *Mater Manuf Process* 9 (1994) 429.
8. S. Zehnder, P. Lorenz, M. Ehrhardt, K. Zimmer, P. Schwaller, *Proceedings of SPIE* 2014; 8967, 89670A.
9. D. Chen, Q. Lu, Y. Zhao, *Appl Surf Sci* 253 (2006) 1573.
10. D. Kim, C. Choi, *J Nanosci Nanotechno* 13 (2013) 7581.
11. X. Peng, K. Jiang, *Advanced Materials Research* 424-425 (2012) 765.
12. A. Focsa, D. Blanc, G. Poulain, C. Barbos, M. Gauthier, N. Quang, M. Lemiti, *Energy Procedia.* 38 (2013) 713.
13. A. Ouchi, Z. Bastl, J. Boháček, J. Šubrt, J. Pola, *Surf Coat Tech* 201 (2007) 4728.
14. F. Kiriakidou, *Catal. Today* 54 (1999) 119.

15. J. Zhu, *Cur. Opin. Colloid Interface Sci.* 14 (2009) 260.
16. K. Kordás, J. Békési, R. Vajtai, L. Nánai, S. Leppävuori, A. Uusimäki, K. Bali, P. Moilanen, *Appl Surf Sci* 172 (2001) 178.
17. H. Hocheng, T. Lin, U. Jadhav, W. Wong, *Microelectron. Eng.* 101 (2013) 17.
18. X. Wang, H. Zheng, G. Lim, *Appl Surf Sci* 200 (2002) 165.
19. V. Kochemirovsky, E. Khairullina, S. Safonov, L. Logunov, I. Tumkin, L. Menchikov, *Appl Surf Sci* 280 (2013) 494.
20. V. Kochemirovsky, S. Safonov, I. Tumkin, Yu. Tver'Yanovich, I. Balova, L. Menchikov, *Russ Chem Bull* 60 (2011) 1564.
21. V. Kochemirovsky, S. Safonov, M. Strukov, I. Tumkin, L. Logunov, L. Menchikov, *Glass Phys Chem* 39 (2013) 403.
22. V. Kochemirovsky, L. Menchikov, I. Tumkin, L. Logunov, S. Safonov, *Quantum Electron* 42 (2012) 693.
23. V. Kochemirovsky, L. Menchikov, A. Kuz'Min, S. Safonov, I. Tumkin, Yu. Tver'Yanovich, *Russ Chem Bull* 61 (2012) 1041.
24. R. J. Von Gutfeld, E. E. Tynan, R. L. Melcher, S. E. Blum, *Appl. Phys. Lett.* 35 (1979) 651.
25. R. E. Acosta, L. T. Romankiw, R. J. Von Gutfeld, *Thin Solid Films* 95 (1982) 131.
26. R. J. Von Gutfeld, K. G. Sheppard, *J. Res. Develop.* 42 (1998) 639.
27. V. Kochemirovsky, S. Fateev, L. Logunov, I. Tumkin, S. Safonov, *Int. J. Electrochem. Sci.* 9 (2014) 644.

© 2015 The Authors. Published by ESG ([www.electrochemsci.org](http://www.electrochemsci.org)). This article is an open access article distributed under the terms and conditions of the Creative Commons Attribution license (<http://creativecommons.org/licenses/by/4.0/>).